

Structural and Morphological Study of W–Sn–O Thin Films Deposited by Rheotaxial Growth and Thermal Oxidation

E. Bontempi,[†] E. Zampiceni,[‡] G. Sberveglieri,[‡] and L. E. Depero^{*,†}

Consorzio Interuniversitario Nazionale di Scienza e Tecnologia dei Materiali and Structural Chemistry Laboratory, Dipartimento di Ingegneria Meccanica, Università di Brescia, Via Branze, 38, 25123 Brescia, Italy, and Istituto Nazionale per la Fisica della Materia and Gas Sensors Laboratory, Dipartimento di Chimica e Fisica, Università di Brescia, Via Valotti, 9, 25123 Brescia, Italy

Received February 11, 2002. Revised Manuscript Received May 16, 2002

In the present paper we analyzed W–Sn–O thin films deposited by the rheotaxial growth and thermal oxidation technique and annealed at different temperatures. The aim of this work is to obtain stable gas sensor materials and to increase the surface-to-volume ratio in the active phase, thus improving the gas sensor sensibility. The structural characterization was performed by means of X-ray diffraction, glancing incidence X-ray diffraction, and X-ray microdiffraction techniques. The morphological characterization was obtained by means of scanning electron microscopy.

Introduction

Transition-metal oxides, such as TiO₂, In₂O₃, SnO₂, and WO₃, are well-known for their high sensitivity to pollution gases. In particular, mixed oxides have recently emerged as promising candidates for gas detection.^{1–2} It was shown that such systems may benefit from the combination of the sensing properties of their components.

Both SnO₂ and WO₃ are well-studied materials in gas sensor research and they have found commercial applications in sensor devices. In particular, SnO₂ is the typical sensing material for air pollution gases³ and WO₃ shows especially high sensitivity to H₂S gas.⁴ Therefore, mixtures of SnO₂ and WO₃ have been suggested as an effective sensing material for monitoring air pollution gases.⁵ Moreover, the ternary Sn_xWO_{3+x} system has widely been studied^{6–8} to characterize the mixed oxides structure.

Some authors⁹ showed that W-doped SnO₂ and WO₃/SnO₂ powders can be employed to obtain gas sensor materials, with sensibility to particular gases, depending on the composition. Indeed, the development of

sensing materials requires an improvement of its characteristics that can be obtained by the introduction of dopants. In particular, the addition of another metal to these oxides can improve the sensibility to specific gases.^{10–13}

It was shown that some additives, such as W, Nb, Mg, and so forth, may stabilize tin dioxide crystalline sites.¹⁴ Then, the presence of metallic additives may modify the crystalline growth kinetics.^{15–17} Recently, Cabot et al.¹⁸ reported the significant microstructural changes induced by platinum and palladium in SnO₂ nanopowders, while Radecka et al.¹⁹ have shown that the rheotaxial growth and thermal oxidation (RGTO) technique produces Sn–Ti–O thin films characterized by extremely rough surfaces.

Sensitivity and selectivity of gas-sensing materials strongly depend also on the synthesis procedure²⁰ because the preparation influences the morphological and structural features, and thus the performance, of the final material.

Searching for new gas-sensing materials must be flanked by a deep study of their structural properties. Indeed, the knowledge of these properties and the

* To whom correspondence should be addressed. E-mail: depero@bsing.ing.unibs.it.

[†] Dipartimento di Ingegneria Meccanica.

[‡] Dipartimento di Chimica e Fisica.

(1) Radecka, M.; Zakrzewska, K.; Rekas, *Sensors Actuators B* **1998**, *47*, 194.

(2) Dusastre, V.; Williams, D. E. *J. Mater. Chem.* **1999**, *9*, 445.

(3) Suzuki, K.; Takada, T. *Sensors Actuators B* **1995**, *24–25*, 773.

(4) Lin, H. M.; Hsu, C. M.; Yang, H. Y.; Lee, P. Y.; Yang C. C. *Sensors Actuators B* **1994**, *22*, 63.

(5) Yun, D. H.; Kwon, C. H.; Hong, H. K.; Shin, H. W.; Kim, S. R.; Lee, K. *Sensors Actuators B* **1996**, *35–36*, 48.

(6) Ekström, T.; Parmentier, M.; Tilley, R. J. D. *J. Solid State Chem.* **1981**, *37*, 24.

(7) Solis, J. L.; Lantto, V. *Sensors Actuators B* **1998**, *48*, 322.

(8) Solis, J. L.; Lantto, V.; Häggström, L.; Kalska, B.; Frantti, J.; Sauko, S. *Sensors Actuators B* **2000**, *68*, 286.

(9) Park, J. H.; Kim, K. H. *Sensors Actuators B* **1999**, *56*, 50.

(10) Cheong, H.; Choi, J.; Kim, H. P.; Kim, J.; Churn, G. *Sensors Actuators B* **1991**, *9*, 227.

(11) Khol, D. *Sensors Actuators B* **1990**, *1*, 158.

(12) Morazzoni, F.; Canevali, C.; Chiodini, N.; Mari, C.; Ruffo, R.; Scotti, R.; Armelao, L.; Tondello, E.; Depero, L. E.; Bontempi, E. *Mater. Sci. Eng. C* **2001**, *15*, 167.

(13) Morazzoni, F.; Canevali, C.; Chiodini, N.; Mari, C.; Ruffo, R.; Scotti, R.; Armelao, L.; Tondello, E.; Depero, L. E.; Bontempi, E. *Chem. Mater.* **2001**, *13*, 4355.

(14) Tao, Z.; Junda, H.; Hong, L. *Appl. Surf. Sci.* **2000**, *161*, 459.

(15) Morrison, S. R. *Sensors Actuators* **1987**, *12*, 425.

(16) Yamazoe, N. *Sensors Actuators B* **1991**, *5*, 7.

(17) Kohl, D. *J. Phys. D: Appl. Phys.* **2001**, *34*, R125.

(18) Cabot, A.; Arbiol, J.; Morante, R.; Weimar, B. N.; Göpel, W. *Sensors Actuators B* **2000**, *70*, 87.

(19) Radecka, M.; Przewoźnik, J.; Zakrzewska, K. *Thin Solid Films* **2001**, *391*, 247.

(20) Lim, C. B.; Oh, S. *Sensors Actuators B* **1996**, *30*, 223.

understanding of their relationship with the annealing treatments are basic for the optimization of reliable gas sensors working at high temperatures. It is very important to notice, for example, that high sensitivities and short response times can be achieved by reducing the particles sizes to nanoscale dimensions. However, the average crystallite size generally increases because of thermal treatments.

In this paper for the first time the preparation and the structural characterization of W–Sn–O thin films deposited by the RGTO²¹ technique are reported. The films were annealed at different temperatures with the aim to investigate structural and morphological properties of these materials.

Experimental Section

Thin film deposition was performed by dc sputtering for Sn and rf sputtering for W in an argon atmosphere with pressures of respectively 2×10^{-3} and 7×10^{-3} mbar. The sputtering plant (Alcatel 450 SCM) operated at 50 W (dc power) for Sn deposition and 150 W (rf power) for tungsten. All the targets are certified by Target Materials Inc. at 99.9% purity. Sn (about 3000 Å) was deposited at 400 °C (temperature higher than that of the melting point), and then without breaking vacuum W (about 160 Å) was deposited at 300 °C.

The calculated deposition rates were 2.7 and 0.32 nm/s for Sn and W, respectively. The final thickness was checked by a profilometer. At 300 °C, the samples were cooled to 100 °C in a vacuum. From 100 °C they were cooled to room temperature for 1 h, in air. Three samples were annealed at 500, 600, and 700 °C, respectively, in oven under a controlled flux of humid synthetic air (70 RH) and the oxidation process was achieved as follows:

- (a) heating from room temperature up to 250 °C at 2 °C/min;
- (b) annealing for 4 h at 250 °C;
- (c) increasing the temperature to the chosen values (500, 600, and 700 °C) at the rate of 1.3 °C/min;
- (d) annealing at this temperature for 30 h;
- (e) cooling to the room temperature (–2 °C/min).

This procedure was adopted to avoid stresses or cracks in the layers and to obtain homogeneous oxidation processes, following RGTO techniques.²²

Scanning electron microscopy (SEM) analyses were performed by a Cambridge Stereoscan 260 microscope equipped with a Link Analytical probe for energy dispersive X-ray spectroscopy (EDXS).

Wide-angle X-ray diffraction (WAXRD) and glancing incidence X-ray diffraction (GIXRD) spectra were collected by a Bruker "D8 Advance" diffractometer equipped with a Göbel mirror. The angular accuracy was 0.001° and the angular resolution was better than 0.01°. The Cu K α line of a conventional X-ray source powered at 40 kV and 40 mA was used and the average crystallite sizes were calculated by means of the Topas P program.²³

The X-ray microdiffraction spectra were collected by a D/max-RAPID Rigaku microdiffractometer. The D/max-RAPID X-ray microdiffractometer with a cylindrical imaging plate (IP) detector can measure two-dimensional (2D) X-ray diffraction from –45° to 160° (2 θ). The irradiated area was 300 μ m.

Discussion

In the present work, we studied the influence of a tungsten overlayer on Sn films structure, microstructure, and morphology. In particular, we report the

results obtained from four samples: one as-deposited (no. 1) and three annealed at 500, 600, and 700 °C (nos. 2, 3, and 4, respectively), as described in the Experimental Section.

In Figure 1a–d SEM micrographs of samples 1, 2, 3, and 4 are reported, respectively.

SEM micrographs show that, after the rheotaxial growth, clusters with semispherical shape are formed (Figure 1a). When this result is compared with that obtained for an undoped Sn thin film,²⁴ the spheres' diameters appear to be smaller, while the grains distribution is in both cases sharp.

When the annealing temperature is increased, the grains morphology always appears compact (Figure 1b–d), even if the grains average dimension is similar in all the samples. Such morphology is responsible for the large surface area obtained for these samples, which is a mandatory condition for semiconductor gas sensor materials because their efficiency is strongly related to surface reactions.

In Figure 2 the SEM micrograph of the pure tin dioxide sample realized with the RGTO technique and annealed at 600 °C²¹ is shown. When the morphologies of the undoped and doped films annealed at the same temperature (600 °C) are compared, it is clear that the W presence inhibits grains agglomeration: in fact, the porous spheres (the sphere surface is spongy) that we obtain in both materials are smaller in the W-doped sample. If the presence of W inhibits the crystalline growth, this material may be a suitable candidate for gas-sensing application.

The decreasing of the W content in the films with the annealing temperature was detected by means of EDXS analysis (see Figure 3). This result may be justified by a possible high volatility of tungsten oxides. Similar effects for Mo–Sn–O thin films were observed.²⁵

In Figure 4 the GIXRD spectra are shown. The incidence angle was fixed at 1°. For sample 1 (Figure 4a), the tin metallic phase was identified (JSPDS,²⁶ card no. 040673), whereas in all the annealed samples SnO₂ cassiterite phase reflections (JSPDS, card no. 710652) and the strongest peak of the SnO phase (JSPDS, card no. 060395) were detected. In the pattern of sample 1 (Figure 4a) the reflections of the tin phase are indicated; no evidence of tungsten phases were found. The intensities ratio of Sn for the peaks 200 (at 2 θ = 30.6°) and 101 (at 2 θ = 32.0°) are different from those calculated from the ideal structure. To verify possible preferred orientation effects, GIXRD patterns for different incidence angles and XRD spectrum were collected. The intensities ratio of peaks 200 and 101 is the same in all the patterns, thus indicating the absence of preferred orientation effects. Then, the difference in the intensities ratio compared to those obtained by the ideal structure can be attributed to the changes of the structural factor of metallic Sn, possibly because of the presence of W in the phase. To the best of our knowledge, this is the first time that this effect is reported. Indeed, nothing similar was found in Mo–Sn–O thin films²⁵ obtained by the

(24) Diéguez, A.; Romano-Rodríguez, A.; Morante, J. R.; Nelli, P.; Sangaletti, L.; Sberveglieri, G. *J. Electrochem. Soc.* **1999**, *146*, 3527.

(25) Bontempi, E.; Zampicini, E.; Sberveglieri, G.; Depero, L. E. *Chem. Mater.* **2001**, *13*, 2608.

(26) JC-PDF database, International Centre for Diffraction Data, 1998.

(21) Sberveglieri, G. *Sensors Actuators B* **1992**, *6*, 239.

(22) Sberveglieri, G.; Faglia, G.; Gropelli, S.; Nelli, P.; Camazi, A. *Semicond. Sci. Technol.* **1990**, *5*, 1231.

(23) Topas P, copyright Bruker AXS Version 1.0.1, 1999.

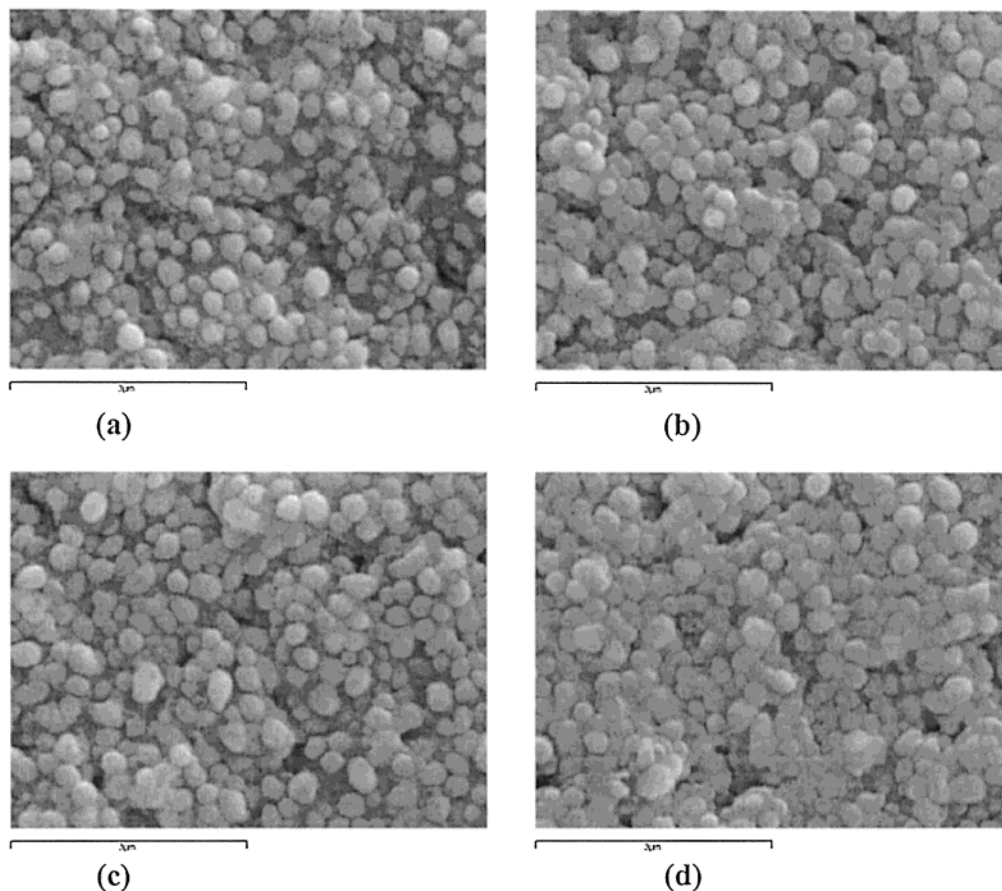


Figure 1. SEM micrographs of the as-deposited (a) and annealed at 500 °C (b), 600 °C (c), and 700 °C (d) samples.

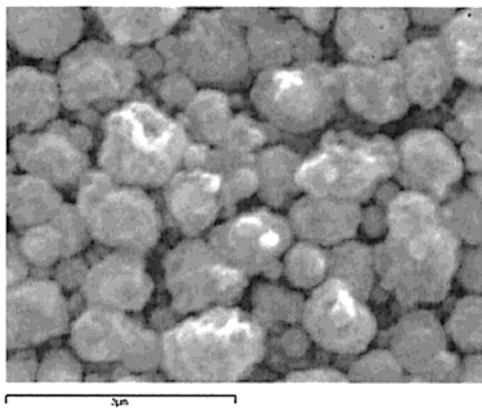


Figure 2. SEM micrographs of the pure tin dioxide (annealed at 600 °C).¹⁴

RGTO technique in which the reflection intensities ratio of the Sn phase was reported in the literature. For all the samples, the crystallite sizes are similar and, on the basis of Scherrer's formula, they were estimated to be about 30 nm.

To check the homogeneity of the films structure, we performed X-ray microdiffraction experiments.

2D patterns obtained in different points of sample 1 show the Debye rings with the same intensity in all directions, confirming the absence of texture in the film (see Figure 5), as previously claimed on the basis of the GIXRD and XRD patterns comparison. However, we obtained slightly different integrated patterns for the selected area.

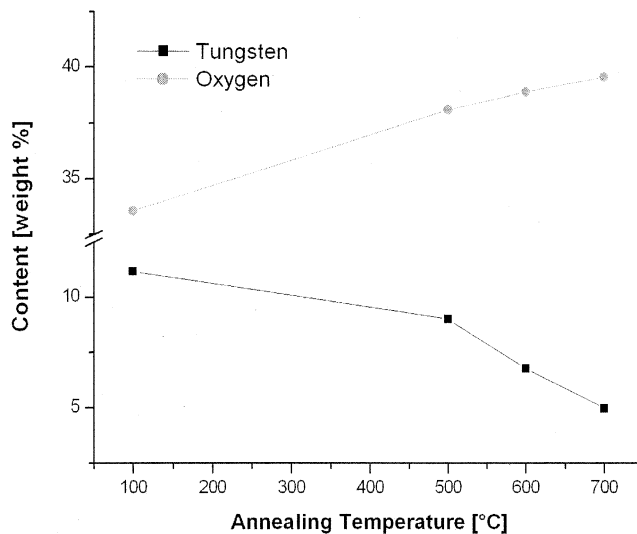


Figure 3. EDXS results: Content, in weight percent, of W and O as a function of annealing temperature.

Indeed, when the intensities of 2D images obtained at two different points were integrated, 2θ patterns were obtained (Figure 6), which can be analyzed by conventional powder diffraction analysis software for phase identification. The 200 and 101 peaks of the tin structure are evidenced in the insets of Figure 6. It is very interesting to notice that whereas the intensities ratio among these peaks as obtained from the pattern of Figure 6 is similar to that found by XRD (Figure 4a), in the pattern of Figure 6a the 200 and 101 peaks intensity

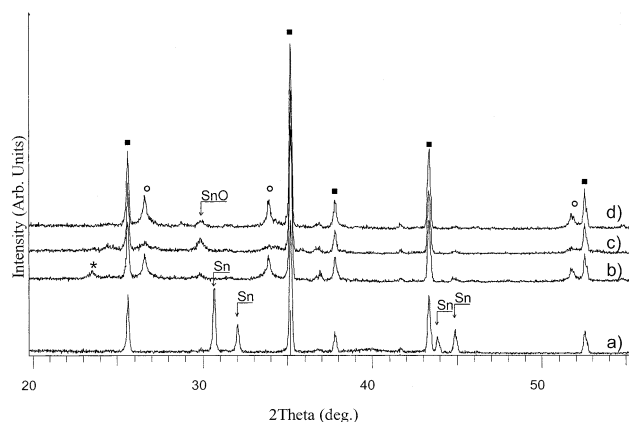


Figure 4. GIXRD spectra of sample 1 (a) (as-deposited), sample 2 (b) (annealed at 500 °C), sample 3 (c) (annealed at 600 °C), and sample 4 (d) (annealed at 700 °C). The glancing incident angle was fixed at 1°. The Al_2O_3 substrate reflections (JSPDS, card no. 711123) are reported (indicated by means of filled squares). The circles indicate reflections attributed to the SnO_2 cassiterite phase. The star indicates the reflection attributed to a tungsten oxide.

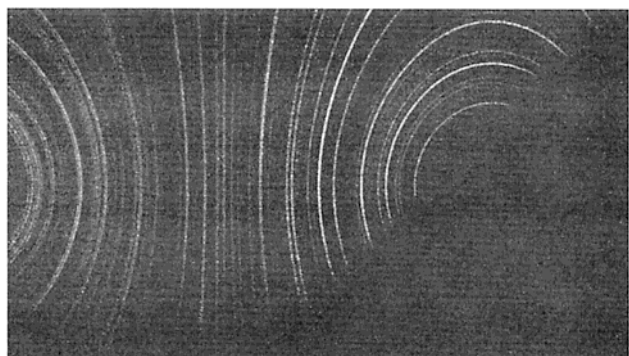


Figure 5. X-ray microdiffraction 2D image, obtained at one point of the as-deposited sample (sample 1), where the absence of preferred orientation is evident. Slightly different patterns were obtained in different areas of the sample. X-ray microdiffraction employs an X-ray beam focused at a spot of 300 μm and is combined with a 2D image-plate detector.

ratio is reversed. This effect was tentatively explained by the presence of different W content inside the Sn structure. Anyhow, we can conclude that the Sn structure of the film before the annealing treatment is not homogeneous.

After the annealing, in addition to Al_2O_3 and SnO_2 cassiterite phases, the peak at $2\theta = 29.9^\circ$ was detected and attributed to the SnO phase (Figure 4b). It was previously reported that during the annealing of RGTO thin films the Sn is partially oxidized to SnO and for a longer annealing time the SnO/Sn ratio increased and finally the cassiterite appeared.²⁷

In the materials studied in the present work, the peak at $2\theta = 24.6^\circ$ may suggest the presence of a small amount of SnO_2 orthorhombic phase.²⁸ This phase, which was detected at high pressures and temperatures, can be structurally related to cassiterite by introducing a periodic microtwinning, as described in refs 29 and 30.

(27) Diéguez, A.; Romano-Rodríguez, A.; Morante, J. R.; Sangaletti, L.; Depero, L. E.; Sberveglieri, G. *Sensors Actuators B* **2000**, *66*, 40.

(28) Mueller, E. *Acta Crystallogr. B* **1984**, *40*, 359.

(29) Depero, L. E.; Perego, C.; Sangaletti, L.; Sberveglieri, G. *Mater. Res. Soc. Symp. Proc.* **1996**, *403*, 577.

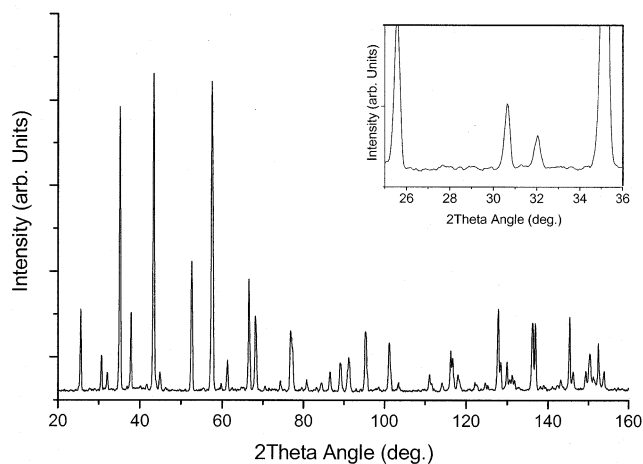
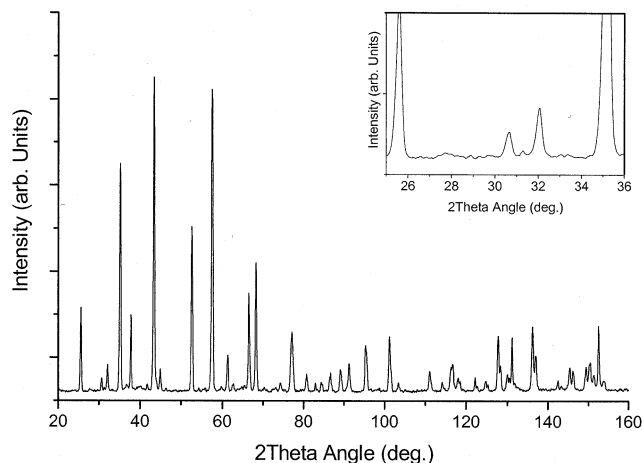


Figure 6. XRD spectra obtained integrating the X-ray microdiffraction 2D measurements from two different areas of the as-deposited sample (sample 1). The insets show, for both the patterns, a magnification of the 2θ area between 25° and 36° containing the 200 and 101 peaks of the tin structure.

Because the reflection at $2\theta = 29.9^\circ$ can be attributed to both the SnO_2 orthorhombic and the SnO phases, it is also possible to suppose that the SnO_2 orthorhombic derives from an oxidation process of SnO. Indeed, it was shown that during the thermal oxidation of Sn, deposited by the RGTO technique, different intermediate SnO_x phases may be obtained.³¹

In sample 2, analyzed after the annealing at 500 °C, a peak at $2\theta = 23.5^\circ$ appears. Any tin oxide has been found to have strong peaks at this position, while there are 22 tungsten oxides having strong peaks at about this value, and among them the strongest reflection has been at 23.5° (2θ). Thus, this reflection was attributed to a tungsten oxide phase, even if the identification was not possible. From this result, we guess that annealing at 500 °C induced the segregation of W oxide.

In samples 3 and 4, where annealing treatments were performed at 600 and 700 °C, respectively, the peak at 23.5° , attributed to the W oxide, can hardly be detected (see Figure 4c,d). This result agrees with the EDXS data

(30) Sangaletti, L.; Depero, L. E.; Diéguez, A.; Marca, G.; Morante, J. R.; Romano-Rodríguez, A.; Sberveglieri, G. *Sensors Actuators B* **1997**, *44*, 268.

(31) Sangaletti, L.; Depero, L. E.; Allieri, B.; Pioselli, F.; Comini, E.; Sberveglieri, G.; Zocchi, M. *J. Mater. Res.* **1998**, *13*, 2457.

previously reported, which suggest a high tungsten oxide volatility.

Even if by XRD no evidence of W substitution in the cassiterite was found in our samples, this cannot be excluded.

Indeed, W substitution in the Sn site of the cassiterite was claimed for W-doped SnO₂ powders prepared by coprecipitation on the basis of the variation of the resistance of W-doped SnO₂ sensing layers with W concentration.⁹ Also in that case the W substitution could not be detected by XRD experiments.

However, in our films the presence of W strongly influenced the morphology: in the W-doped SnO₂ films the growth of the grains was inhibited with respect to pure SnO₂ film. This effect was already reported³² for W-implanted SnO₂ multilayer thin films.

Conclusions

In this paper, we reported the structural and morphological features of W–Sn–O thin films, deposited,

(32) Tao, Z.; Tonghe, Z.; Huixing, Z.; Benkun, M.; Xiaoj, Z.; Kan, X.; Junda, H.; *Nucl. Instrum. Methods Phys. Res., Sect. B* **1998**, *135*, 560.

for the first time, by the RGTO technique and the effects of thermal treatments at different temperatures. We showed that the process oxidation of the W–Sn–O is rather complex: the resulting phase transitions are quite different with respect to that obtained for the previously studied SnO₂ thin films.^{14,25} In particular, the RGTO technique allowed production of W–Sn–O microspheres homogeneously dispersed on the substrate surface. The main effect of W is to stabilize the spheres dimension at about 30 nm, thus being lower compared to that obtained for undoped SnO₂ thin films. The small dimensions of the grains determined at a high surface area. The structural results, showing the presence of substitutional W in the Sn structure are obtained also by means of the X-ray microdiffraction technique.

Acknowledgment. Part of this work has been financially supported by CNR Progetto Finalizzato MSTAI.

CM0201201